Gas Ionization and Magnetic Field Coupling in B335

CEA-ICE

Victoria Cabedo (ICS, HWU)

A. Maury, J.M. Girart, M. Padovani, P. Hennebelle, M. Houde & Q. Zhang

November 10th, 2022

Introduction

CR in the low-mass star formation process

- Why CRs? → Ionization degree
  - Chemistry (ion chemistry, ice chemistry, metal catalysis…)
  - Magnetic field coupling (magnetic braking catastrophe)

Introduction

CR in the low-mass star formation process

- Why CRs? → Ionization degree
  - Chemistry (ion chemistry, ice chemistry, metal catalysis…)
  - Magnetic field coupling (magnetic braking catastrophe)
- Where do they come from?
  - Galactic CRs
  - Local CRs

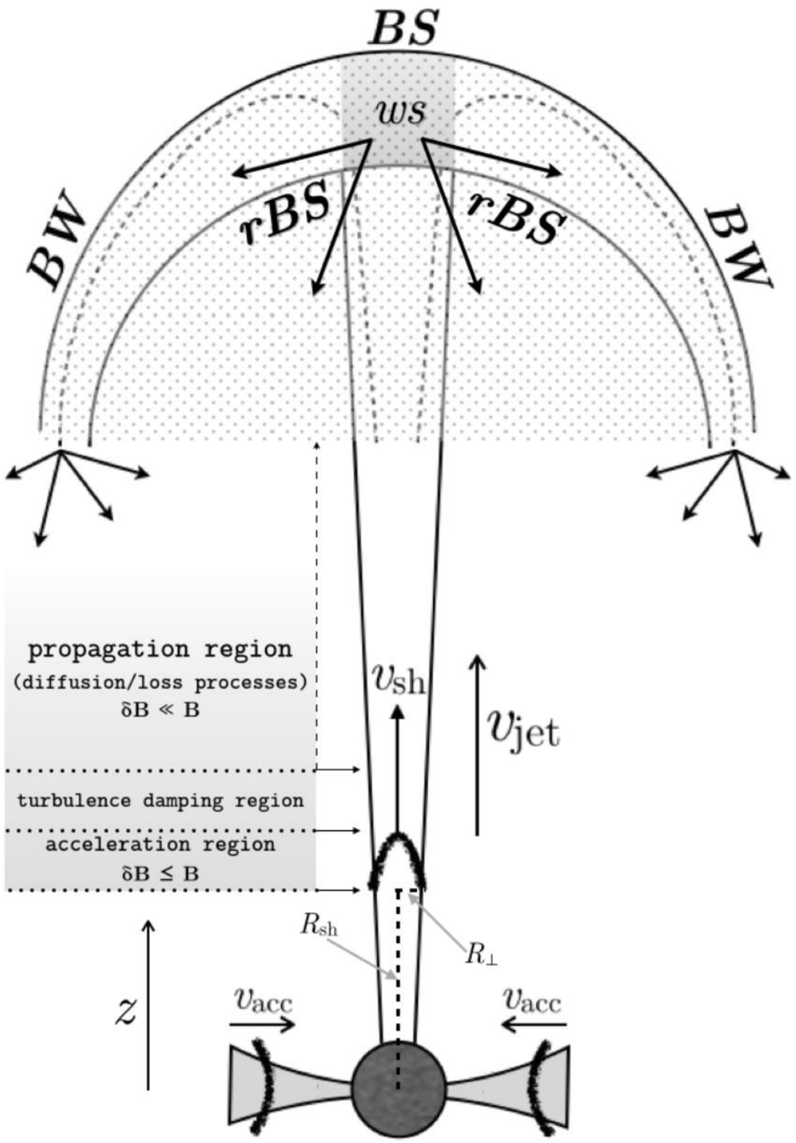

(Padovani+2016)

Introduction

CR in the low-mass star formation process

- Why CRs? → Ionization degree
  - Chemistry (ion chemistry, ice chemistry, metal catalysis…)
  - Magnetic field coupling (magnetic braking catastrophe)
- Where do they come from?
  - Galactic CRs
  - Local CRs
- How do we measure it?
  - https://doi.org/10.1051/0004-6361/202243813

Introduction

The method

Characterize the level of ionization at small envelope radii

- We followed the method by Caselli+1998:
  - The deuteration fraction, R_D, is related to the ionization fraction, χ_e, by *(Wootten+1979, Caselli+1998)*:

$$\chi_e = \frac{2.7x10^{-8}}{R_D} - \frac{1.2x10^{-6}}{f_D}$$

  - And the CR ionization rate is:

$$\zeta = \left[7.5x10^{-4}\chi_e + \frac{4.6x10^{-10}}{f_D}\right]\chi_e n_{H2} R_H$$

(Maury+, 2018)

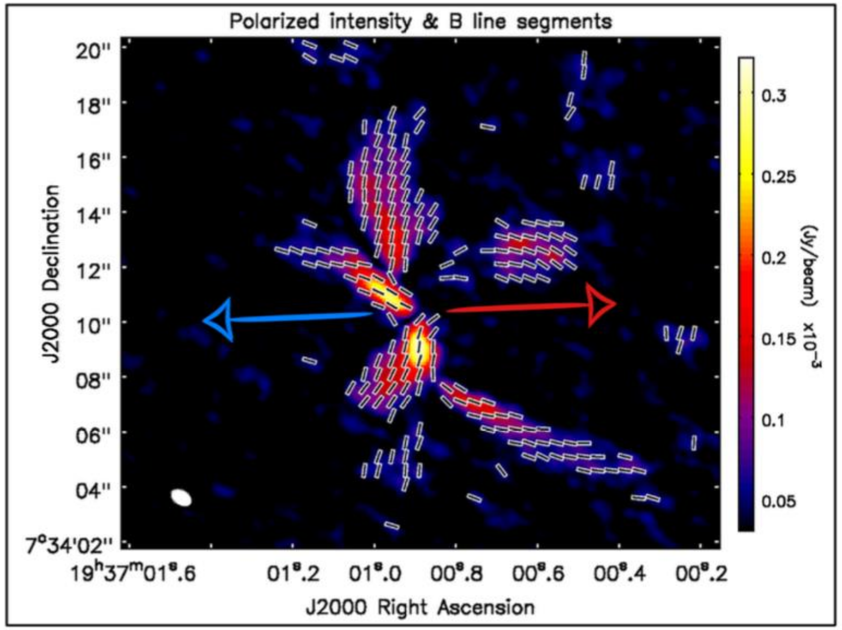

Introduction

The Class 0 Protostar B335

- Isolated Bok globule with a Class 0 protostar at 164.5 pc *(Keen, 1983; Watson, 2020)*
  - Harbours a hot corino *(Imai+, 2016)*
  - W-E CO Outflow *(Hirano+, 1988&1992)*
  - Non-symmetric motions and possible preferential accretion *(Cabedo+, 2021b)*
- Magnetically regulated collapse
  - No disk of more than 10 AU *(Yen+, 2015)*
  - Polarised dust emission shows organised magnetic field *(Maury+, 2018)*

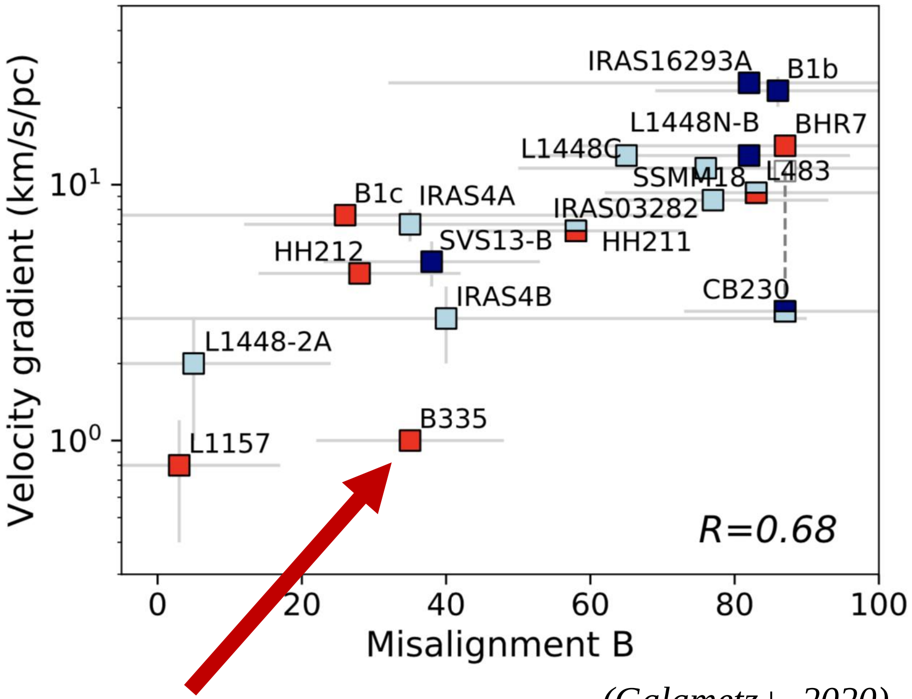

(Galametz+, 2020)

ALMA Observations

Molecular lines

- High angular resolutions observations of molecular lines on B335.
  - Angular resolution = 0.8 – 2.6 arcsec
  - Spectral resolution ≈ 0.2 km/s.
- Beam matching maps

	DCO^+ (J=3-2)	$H^{13}CO^+$ (J=3-2)	^{12}CO (J=2-1)	N_2D^+ (J=3-2)	$H^{13}CO^+$ (J=1-0)	$C^{17}O$** (J=1-0)	cont.
Rest. Freq. (GHz)	216.112	260.255	230.538	231.321	86.754	112.359	110
Θ_{LRS}* (arcsec)	11.3	16.0	10.6	10.6			22.3
Pixel size (arcsec)	0.5	0.5	0.5	0.5	0.25	0.25	0.3
Θ_{maj} (arcsec)	1.5	1.5	1.5	1.5	2.6	2.6	0.8
Θ_{min} (arcsec)	1.5	1.5	1.5	1.5	2.6	2.6	0.7
P.A. (°)	0	0	0	0	0	0	−61.5
Spectral res. (km s^{-1})	0.2	0.2	0.2	0.2	0.15	0.15	-
rms (mJy $beam^{-1}$)	22.37	53.15	143.5	6.00	18.58	10.57	0.065
vel. range (km s^{-1})	7.8 - 8.9	7.5 - 8.9	7.6 - 9.4	7.7 - 8.9	7.4-9.2	4.7-6.5 7.7-9.3	-
rms (mJy $beam^{-1}$ km s^{-1})	11.17	21.28	634.6	5.23	17.17	17.58	-

* Largest recoverable scale, computed as $\Theta_{LRS} = 206265(0.6\lambda/b_{min})$ in arcsec, where λ is the rest wavelength of the line, and b_{min} is the minimum baseline of the configuration, both in m (Asayama et al. 2016).
** The two velocity ranges correspond to the two resolved hyperfine components.

ALMA Observations

Molecular lines

- High angular resolutions observation
  - Angular resolution = 0.8 – 2.6 arcsec
  - Spectral resolution ≈ 0.2 km/s.
- Beam matching maps
- Spectral maps

ALMA Observations

Molecular lines

- High angular resolutions observ
  - Angular resolution = 0.8 – 2.6 arc
  - Spectral resolution ≈ 0.2 km/s.
- Beam matching maps
- Spectral maps
- Integrated intensity maps

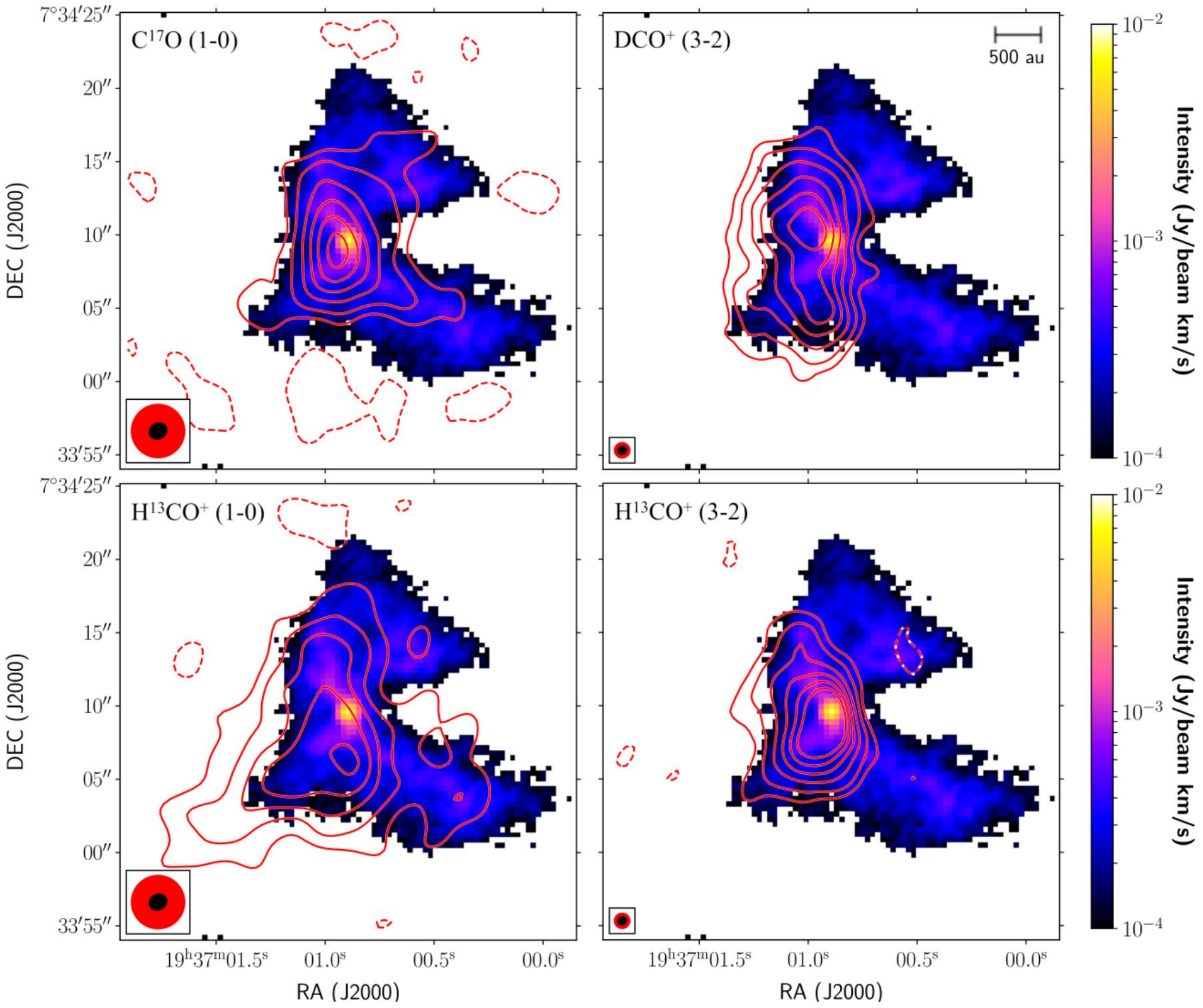

Integrated intensity maps for each tracer (in red contours), superimposed over the cont. intensity @110 GHz. Contours show emission for -2, 3, 5, 8, 11, 14 and 17σ

ALMA Observations

Molecular lines

- High angular resolutions observa
  - Angular resolution = 0.8 – 2.6 arcs
  - Spectral resolution ≈ 0.2 km/s.
- Beam matching maps
- Spectral maps
- Integrated intensity maps
- Molecular line profiles modelling
  - *Hfs* fitting (*Estalella+2017*)
  - 2 velocity components
  - Peak velocity, velocity dispersion and intensity maps

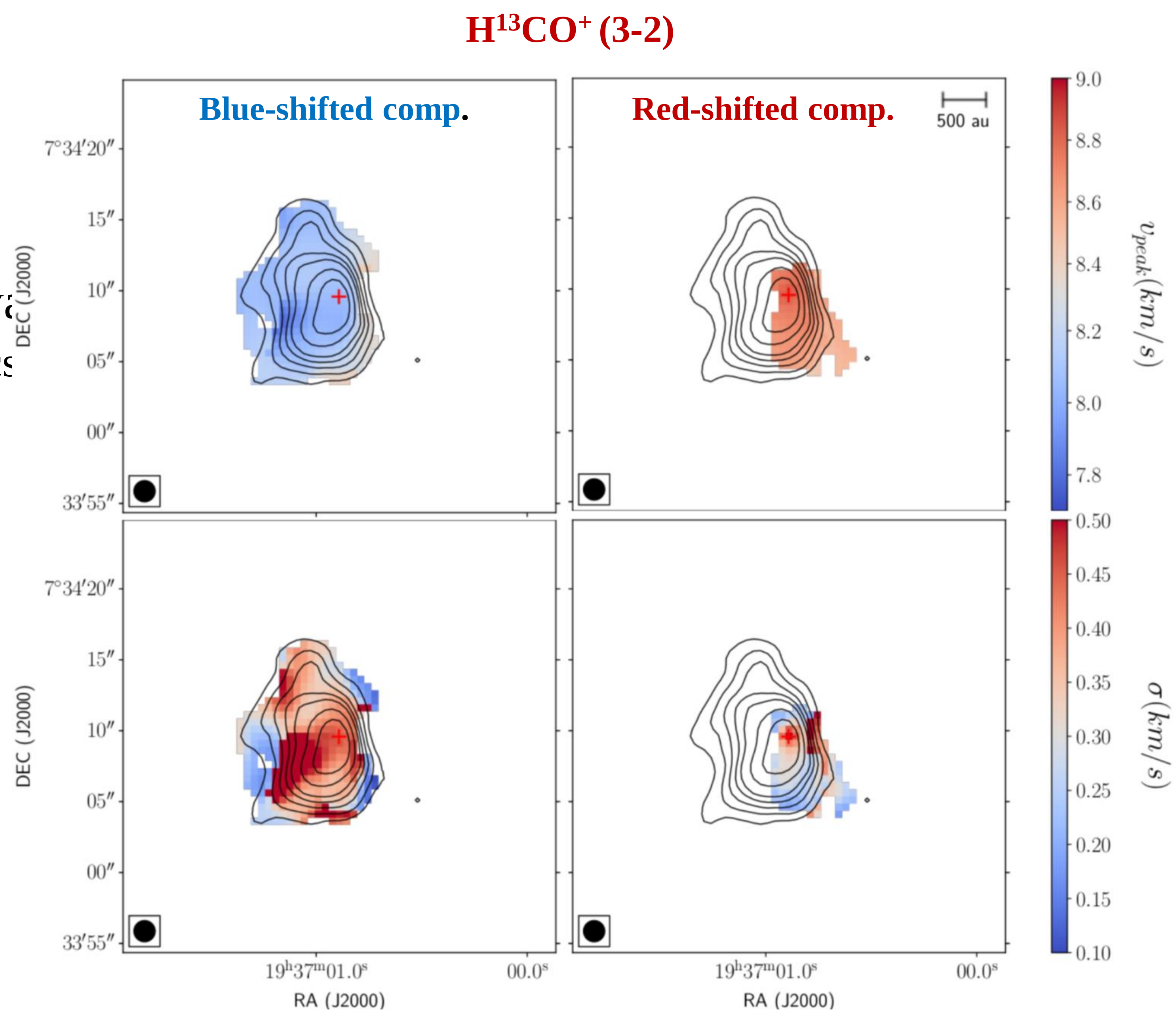

Deuteration Fraction
R_D

- R_D is the column density ratio, accounting for the abundance ratio of ^{12}C to ^{13}C ($f_{12/13C} = 43$):

$$R_D = \frac{1}{f_{12/13C}} \frac{\chi\,(DCO^+)}{\chi\,(H^{13}CO^+)}$$

- R_D ranges from **~0.25 %** to **~2 %**

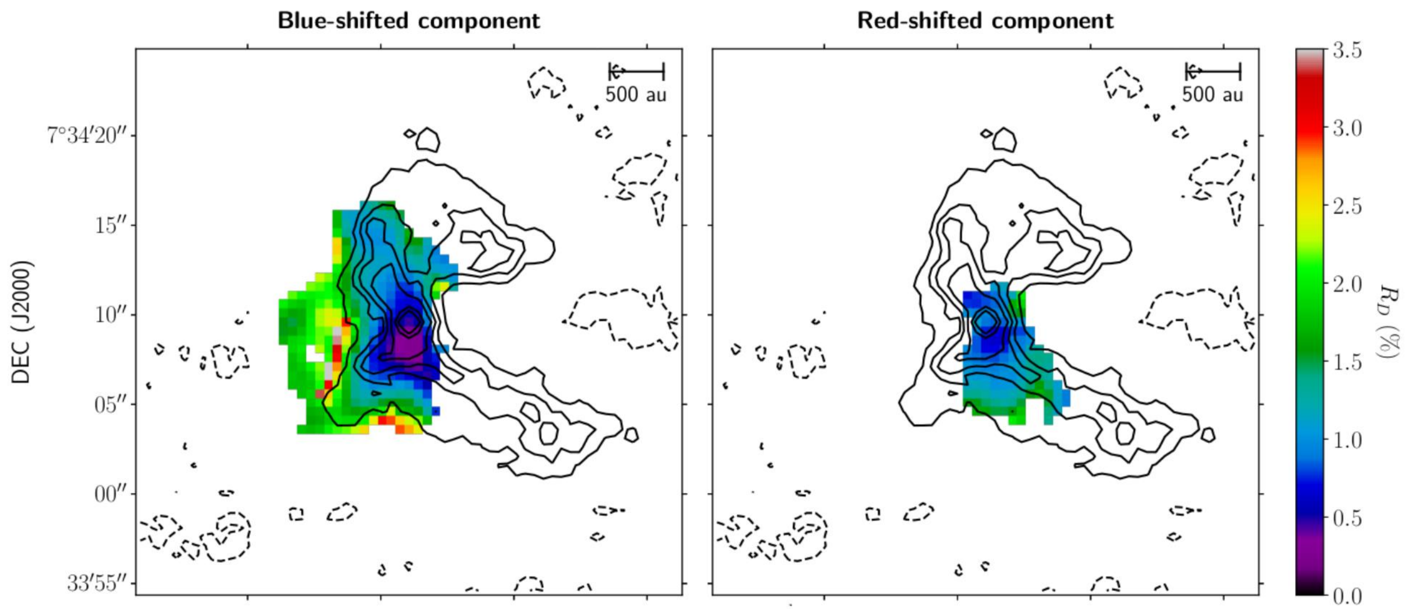

Deuteration fraction (in %), superimposed with dust cont. emission @110 GHz, for emission at -2, 3, 5, 7, 10, 30 and 50σ

Deuteration Fraction

R_D

- R_D is the column density ratio, accounting for the abundance ratio of ^{12}C to ^{13}C ($f_{12/13C} = 43$):

$$R_D = \frac{1}{f_{12/13C}} \frac{\chi\,(DCO^+)}{\chi\,(H^{13}CO^+)}$$

- R_D ranges from **~0.25 % to ~2 %**
- Deuteration decreases towards small scales (0.25% to 3 %, *Butner+, 1995*)

→ **Local destruction of deuterated molecules**

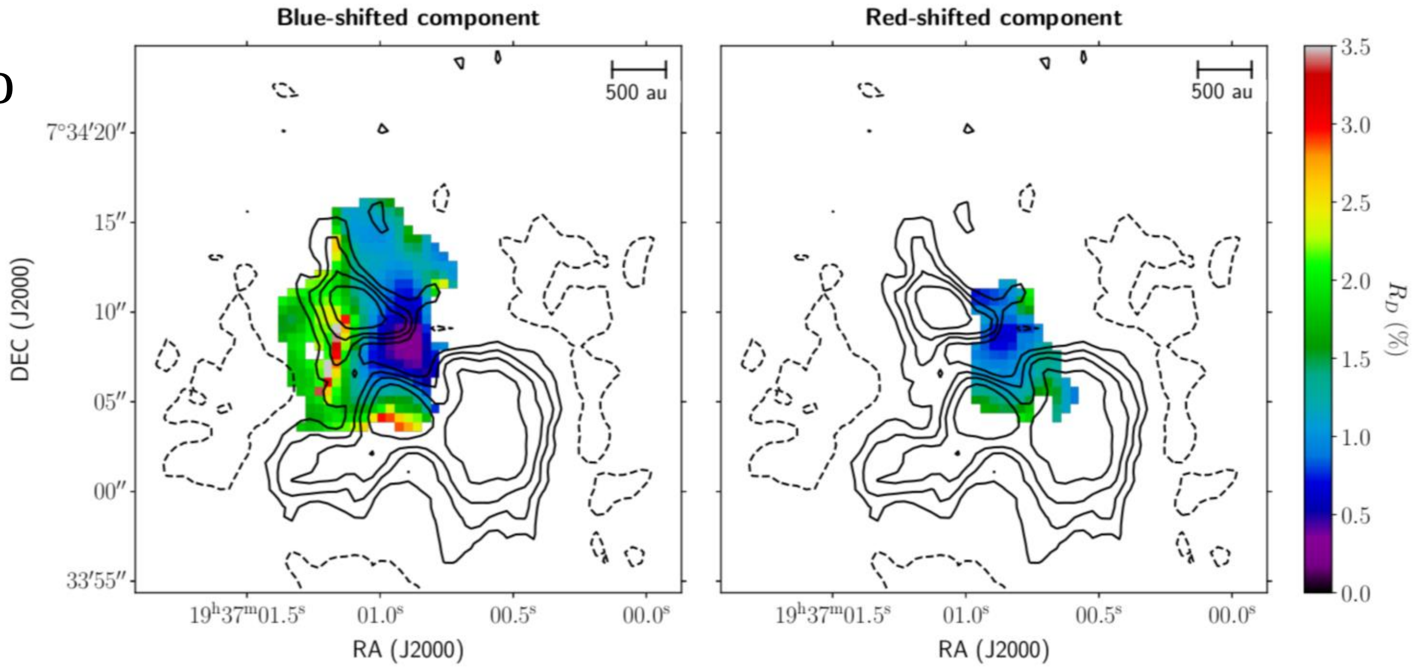

Deuteration fraction (in %), superimposed with N2D+ (3-2) emission, for -3, 3, 5, 10, 15 and 20σ

Ionization Processes

Depletion Factor, f_D

- f_D is the 'expected' CO abundance vs. the 'observed' CO column density, computed as:

$$f_D = \frac{N_{H2} X_{CO}}{N_{C17O} f_{C17O}}$$

- **High depletion values (20-70), highly asymmetric and increasing towards the centre**
- High depletion regions coincide with low deuteration regions

Depletion factor, superimposed with dust cont. emission @110 GHz, for emission at -2, 3, 5, 7, 10, 30 and 50σ

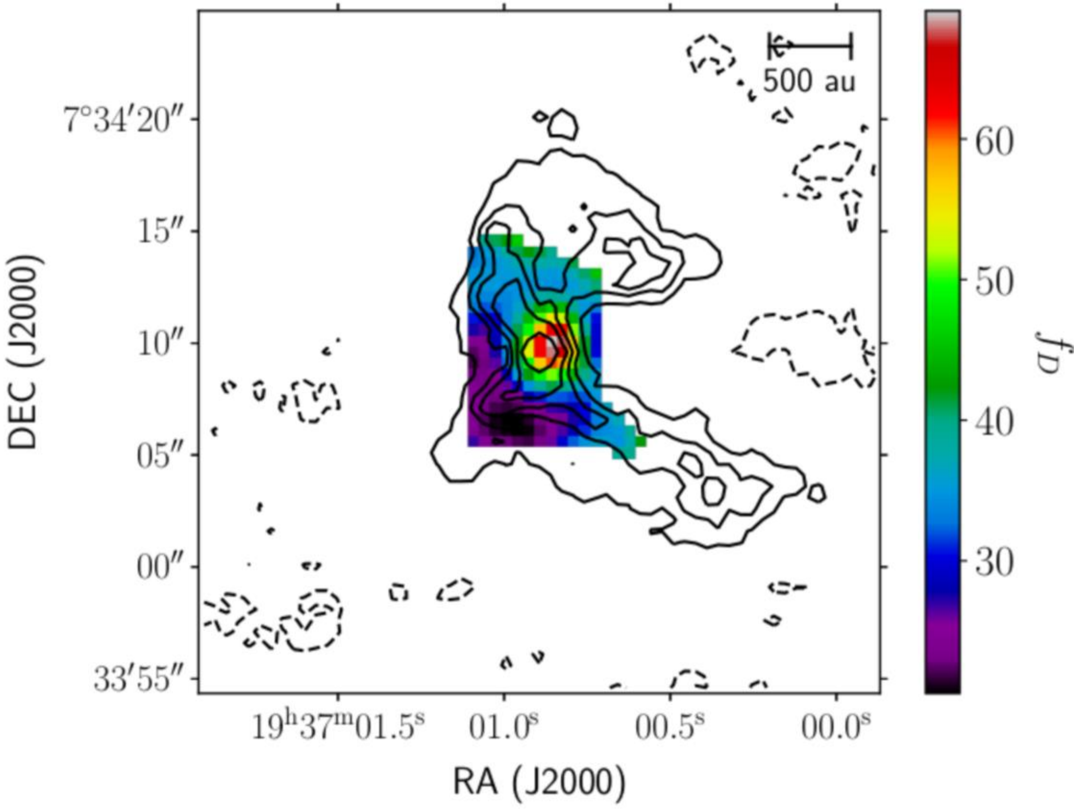

Ionization Processes

Depletion Factor, f_D

- f_D is the 'expected' CO abundance vs. the 'observed' CO column density, computed as:

$$f_D = \frac{N_{H2}\, X_{CO}}{N_{C17O}\, f_{C17O}}$$

- **High depletion values (20-70), highly asymmetric and increasing towards the centr**
- High depletion regions coincide with low deuteration regions

Depletion factor, superimposed with dust cont. emission @110 GHz, for emission at -2, 3, 5, 7, 10, 30 and 50σ

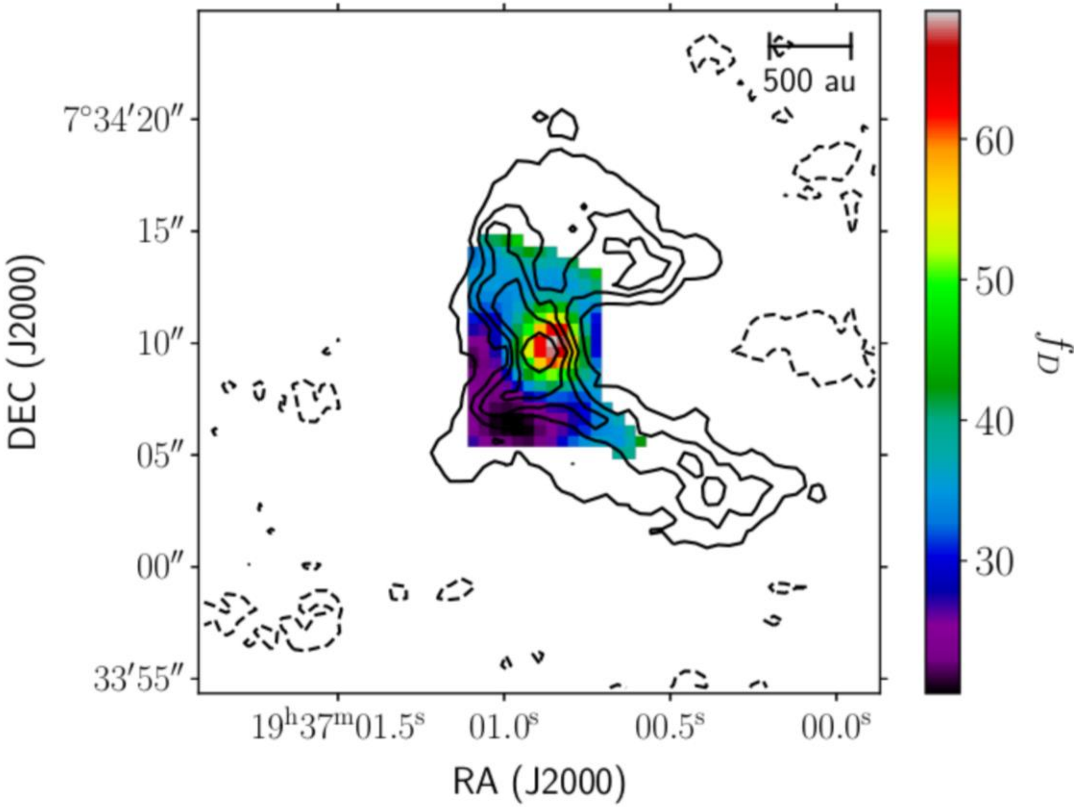

- Not due to CO freeze-out, T ~ 20-30 K *(Walmsley+1987; Murphy+1998)*:
  - CO conversion to CH_3OH and CH_4 *(Aikawa+, 2012)*
  - **CO photodissociation by local radiation processes and conversion to HCO^+ *(Visser+, 2009)***

Ionization Processes

Ionization Fraction, χ_e

- Large ionization fraction, $\chi_e = \mathbf{2x10^{-6}}$
- The ionization basically depends on the **level of deuteration,** not the depletion factor
- **χ_e increases towards the centre**

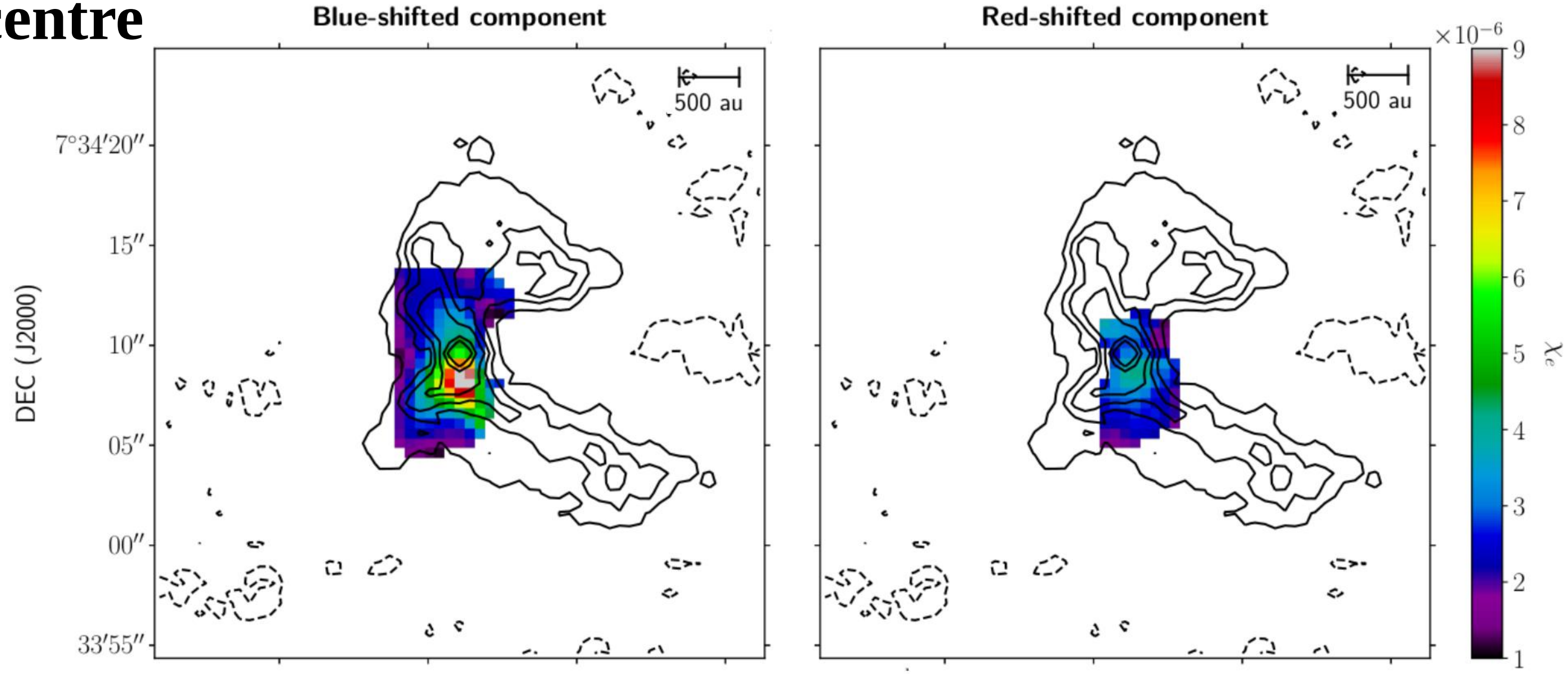

Ionization fraction, superimposed with dust cont. emission @110 GHz, for emission at -2, 3, 5, 7, 10, 30 and 50σ

Ionization Processes

CR Ionization Rate, ζ

- ζ mostly depends on χ_e
- ζ increases towards the centre, reaching values of $\boldsymbol{7x10^{-14}\ s^{-}}$ **at the protostar position**

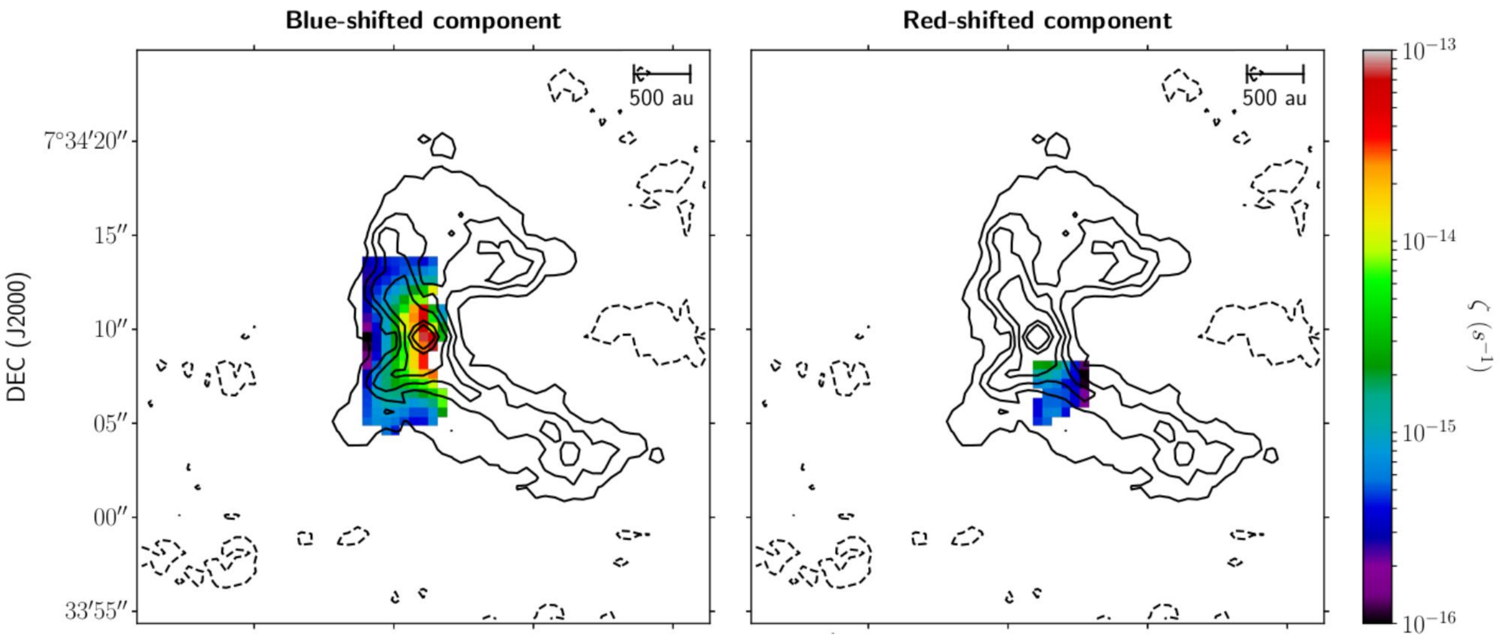

CR ionization rate, superimposed with dust cont. emission @110 GHz, for emission at -2, 3, 5, 7, 10, 30 and 50σ

Ionization Processes

CR Ionization Rate, ζ

- ζ mostly depends on χ_e
- ζ increases towards the centre, reaching values of $\mathbf{7x10^{-14}\ s^{-}}$ **at the protostar position**
- Not compatible with ionization→ **Local ionization processes?**

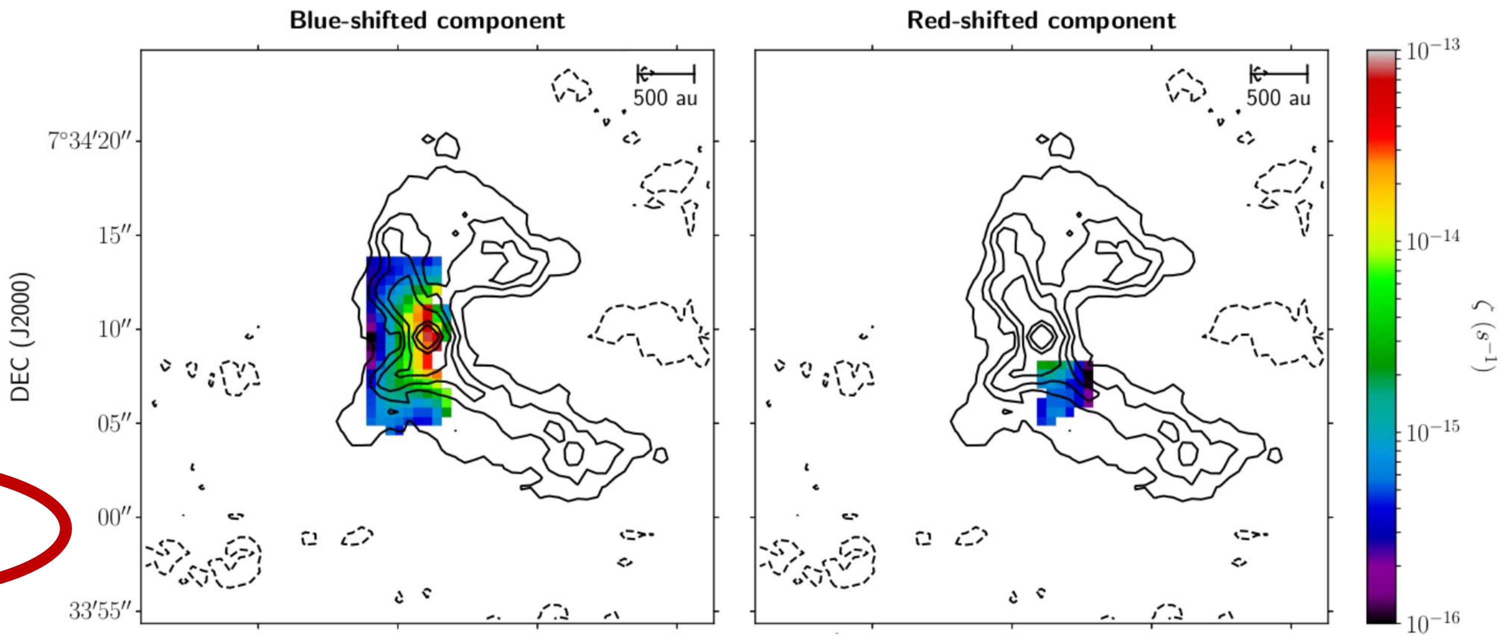

CR ionization rate, superimposed with dust cont. emission @110 GHz, for emission at -2, 3, 5, 7, 10, 30 and 50σ

Origin of the ionization

Local CR acceleration

- No far-UV or X-Ray radiation

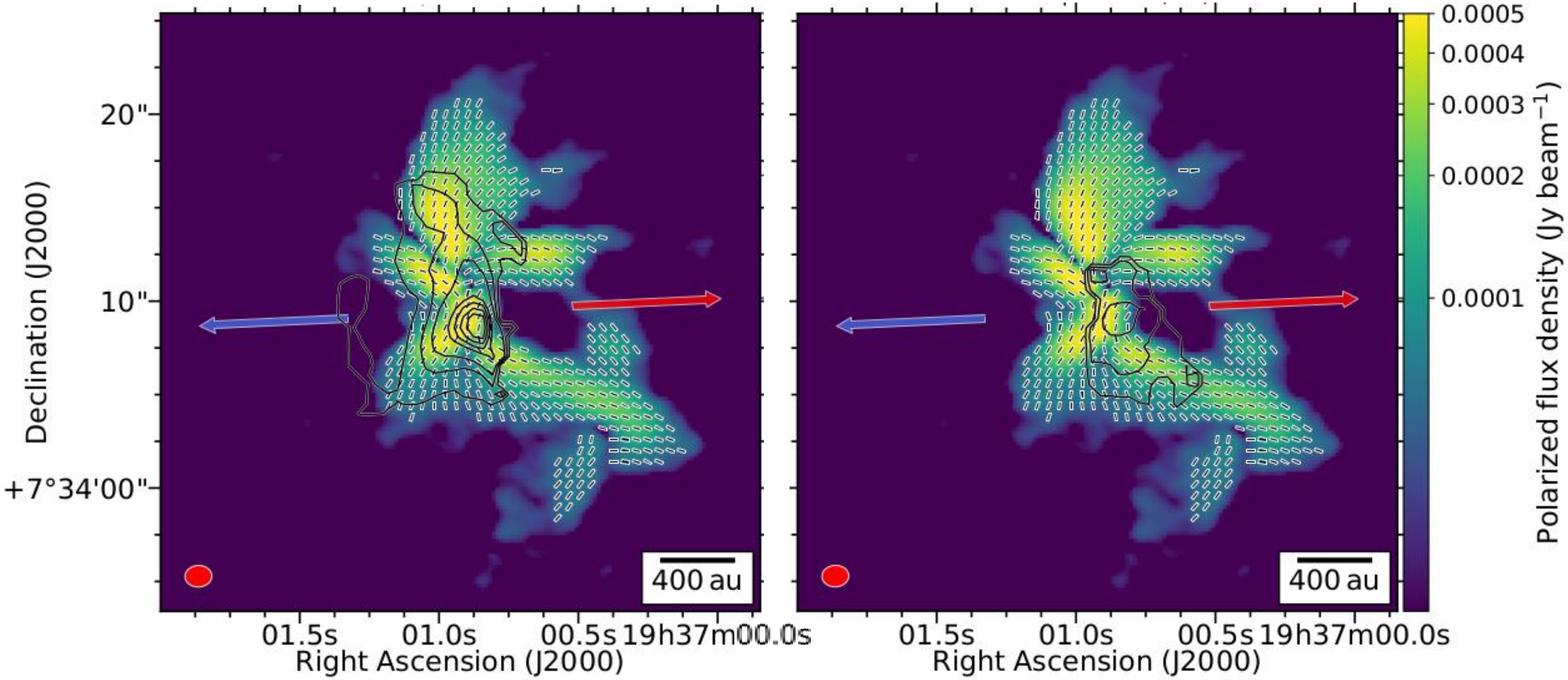

Rd vs. B field morphology

Origin of the ionization

Local CR acceleration

- No far-UV or X-Ray radiation

- Local CR acceleration can have two origins:
  - **Strong magnetized shocks along the outflow** *(Padovani+, 2015&2016; Fitz Axen+, 2021; Padovani+, 2021)*
  - **Accretion shocks near the protostellar surface** *(Padovani+, 2016; Gaches+, 2018)*

- B335 hosts a powerful jet *(Galfalk+, 2007; Yen+, 2010)*

- B335 exhibits an organized magnetic field at small scales *(Maury+, 2018)*

Origin of the ionization

Ionization trend

- We measure $\zeta(\bar{r}, \vartheta)$, where $\bar{r}$ is the ζ average at different radii, for the different angles, $0 \leq \vartheta \leq \pi$

- Two power-law profiles $\zeta \propto r^s$:
  - **Inner envelope (< 270 AU)**
    $s = -0.96$
    Compatible with CR diffusive regime ($s = -1$)
  - **Outer envelope (> 270 AU)**
    $s = -3.77$
    CRs are thermalized?
    Symmetry is lost?

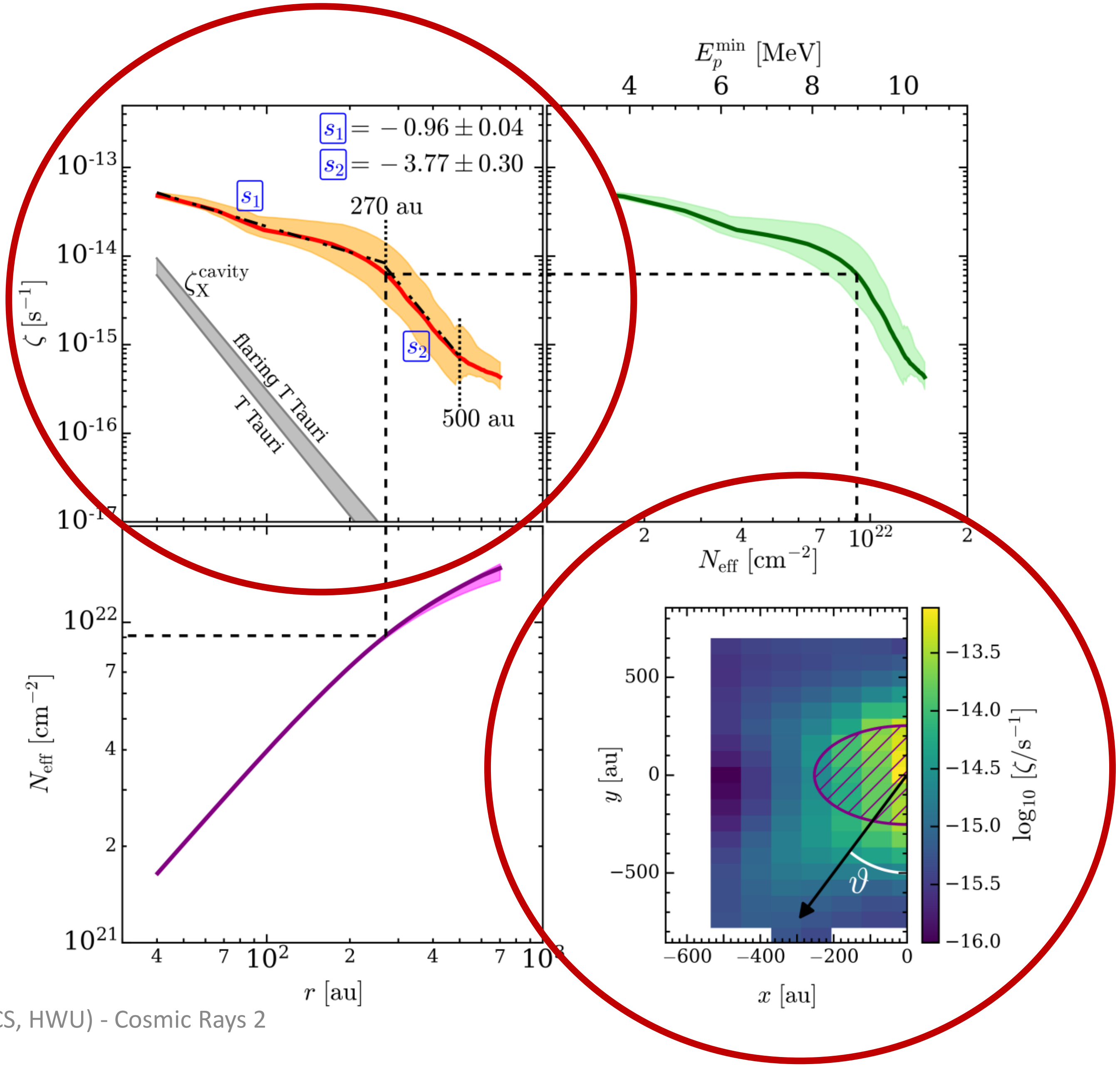

Caveats of the method

Is this correct?

- The bad:
  - Uncertainties are large:
    - Uncertainties from the data
    - Uncertainties in the parameters: T_{dust}, T_{ex}, dust opacity…
  - Is there chemical equilibrium?

- The good:
  - Relation between ζ and R_D is better if ionization is high *(Shingledecker+,2016; Bron+,2021)*
  - H_3^+ methods underestimate ζ, except where CR ionization dominates *(Gaches+, 2019)*
  - Models including protostellar sources predict such CRIR *(Gaches+,2018; Gaches+,2019)*
  - Corrections are important at $R_D > 10\%$ *(Bovino+, 2020)*

The implications

Ionization and B field coupling

- The ionization fraction of the gas determines:
  - The coupling between the gas and the B field
  - The role of diffusive processes, such as ambipolar diffusion

- **The large ionization in B335 should lead to an almost perfect coupling, producing strong magnetic braking**
  - This supports previous observations on B335 *(Yen+, 2015; Maury+, 2018)*

- **Change from non-ideal MHD to ideal MHD conditions** during the first stages of protostellar formation
  - Disk properties might be determined by local ionization conditions *(Kuffmeier+, 2020)*

Conclusions

- Derivation of χ_e and ζ maps at small scales (< 1000 AU) in the Class 0 protostar B335
  - Values of χ_e are larger than typically measured in protostars ($\chi_e = 1 \sim 7x10^{-6}$)
  - Maps suggest very high values of ζ and increasing towards the centre

    →Local production of CRs
  - Efficient coupling between the gas and the B field leading towards a an important magnetic braking
- **More observations at larger angular resolution and of a larger sample of protostars are needed to confirm the results:**

Astrocatalysis @ ICS, HWU

***In Operando* Studies of Catalysis and Photocatalysis of Space Abundant Transition Metals**

- 4 years project: HWU (Edinburgh) + UAB (Barcelona) + FHI (Berlin)

Our 'Astro Miller-Urrey' Experiment:

1. Replicating interstellar dust metallic inclusions *(Cabedo+, 2021a;* https://doi.org/10.1051/0004-6361/202039991*)*
2. Thermal and photo-induced chemistry on catalytic systems at different astrophysical conditions during the SFP
   - Including S and P chemistry!!
3. Parallel chemical modelisation of the observed reactions

Many thanks!

Other questions:
v.cabedo@hw.ac.uk